A predictive model for the estimation of the deflagration index of organic dusts

Sabrina Copelli[a]*, Marco Barozzi[a], Martina Silvia Scotton[a], Anna Fumagalli[b], Marco Derudi[c], Renato Rota[c]

[a] Università degli Studi dell'Insubria - Dip. di Scienza e Alta Tecnologia - via G.B. Vico 46 – 21100 Varese – Italy

[b] DEKRA - Via Fratelli Gracchi 27 - Torre Sud 20092 Cinisello Balsamo (MI) - Italy

[c] Politecnico di Milano - Dip. di Chimica, Materiali e Ingegneria Chimica "G. Natta" - via Mancinelli 7 – 20131 Milano – Italy

*to whom correspondence should be addressed – fax +390332218780; e-mail: sabrina.copelli@uninsubria.it

Abstract

Among all the powder handling operations, the hazard represented by organic dusts explosions is one of the most critical, as several industrial accidents occurred during the last centuries testify. Particularly, in order to estimate the magnitude of a dust explosion, the so-called deflagration index, K_{St}, plays a fundamental role because it is also used to design the emergency vents aimed to protect both vessels and silos from a collapse due to an internal explosion. Nowadays K_{st} values are obtained by means of experimental testing, e.g. using a standard 20 L sphere, but its determination is quite expensive and time consuming. This problem is even more severe when a target dust is processed into a plant giving rise to a wide range of particles sizes; in this case, an experimental investigation of all the different granulometries would be advisable but too expensive. In this context, the aim of this work was to develop a predictive model for the evaluation of the K_{St}, for whatever organic dust, as it would be estimated by a standard test in the 20 L sphere using only a single thermo-gravimetric test. In order to validate the aforementioned model, eight different organic dusts (Aspirin, Cork, Cornstarch, Niacin, Polyethylene, Polystyrene, Sugar, and Wheat Flour) were tested. Preliminary results showed a good agreement between literature K_{St} values and model predictions. Such an achievement, once further validated on a wider range of explosive organic dusts, could lead to an improvement in the risk assessment panorama for powder handling operations by making the risk evaluation process quicker and cheaper.

Keywords: Organic Dusts; Deflagration Index Estimation; Explosion Severity; Dust Explosion Modeling; Powder Handling Operations Safety.

1. Introduction

Risk mitigation in workplaces is becoming an issue of paramount importance, especially with regard to both industrial processes and powder handling operations (Copelli et al., 2017a) involving potentially serious consequences for human health and infrastructures. Surely, among all powder handling operations, the hazard represented by organic dusts explosions is one of the most critical, as several industrial accidents occurred during the last centuries testify. In 2017, there were 68 dust explosions mainly due to organic powders (Cloney, 2017), which caused several injuries and fatalities. Hence, the correct design of the explosion protections becomes very important with the aim of managing properly the explosions that may occur in the industrial plants, thus limiting the personnel involved and the damages to the installation or its equipment.

The main parameters used during the protection design are the maximum explosion overpressure (P_{max}) and the dust deflagration index (K_{St}). In particular, the dust deflagration index is directly related through the so-called "Cubic Law" (Bartknecht, 1971, 1978) to the maximum rate of pressure rise, which is a measure of the violence of explosions.

The maximum values of the above mentioned explosion data are determined so far experimentally in specific vessels with an ignition source approximately positioned in the center. In the 1 m^3 ISO vessel, specified by the International Standards Organization (ISO, 1985), the dust is stored in a 5 liters vessel under a 20 bar air pressure before to be dispersed in the main chamber through a perforated pipe and, after a specific delay time, ignited. The ignition source involves chemical ignitor of 10 kJ but, considering the large vessel size, their influence is small. On the other hand, the dust concentration distribution inside the vessel is not known (Eckhoff, 2003).

Data obtained using the 1 m^3 apparatus are considered representative of the real effects generated by a dust explosion in industrial equipment. However, the amount of dust required by the test is significant and a lot of time is necessary to carry out a complete dust characterization; moreover, cleaning operations can be quite cumbersome in standard laboratories.

Hence, different type of lower volume equipment has been investigated in order to make these evaluations

more affordable. Several investigations have shown that explosions data obtained in smaller vessels can be used to evaluate both P_{max} and K_{St} with some limitations.

These investigations demonstrated that combustible dusts need a minimum volume, variable according to the explosion violence, to develop completely the velocity of the combustion reaction. Indeed, only the parameter P_{max} remains constant with a volume change; instead, the deflagration index needs to be determined by a minimum volume of about 16 litres (Bartkencht, 1981). This leads to the evidence that the violence of the explosion, expressed through the deflagration index (K_{St}), is one of the most difficult parameters to be evaluated.

Nowadays, the most used apparatus is the 20 litres sphere developed by Siwek (1977). This device is able to reproduce with a good accuracy the experimental data of the 1 m^3 ISO vessel (ISO, 1985) using a rebound nozzle, which is a particular dispersion system (Siwek, 1988).

Basing on the promising results of the Siwek apparatus, in recent years, several authors have proposed different approaches trying to reproduce the 20 L sphere experimental data (Fumagalli et al., 2016; Beidaghy et al., 2014). However, a general mathematical method to evaluate the deflagration index has not been proposed yet.

Therefore, the aim of the present work was to develop and validate a mathematical model able to predict the value of the deflagration index, for a given organic powder, as it could be estimated using a standard test in the 20 L sphere. For each analyzed dust, the model requires the estimation of a lumped devolatilization chemical kinetics through a single thermo-gravimetric (TG) experimental test. In order to validate the developed model, eight different organic dusts were analyzed: Aspirin, Cork, Cornstarch, Niacin, Polyethylene, Polystyrene, Sugar, and Wheat Flour. The comparison among experimental and estimated K_{St} values is very promising as the model predictions were found to be always both in the acceptability range related to the unavoidable experimental uncertainties.

2. Mathematical model

For organic dust clouds, devolatilization followed by gas-phase combustion can be proposed as the dominant mechanism of flame propagation (Eckhoff, 2003, Cashdollar et al., 1989, Hertzberg and Zlochower, 1990).

However, as discussed in details elsewhere (Fumagalli et al., 2017), an unusual description of the ignition phenomena arising in the 20 L sphere has been used. In particular, based on several experimental evidences, it has been assumed that the ignitors bursting creates a sort of fireball inside the sphere at a time scale much lower than that of the dust combustion. Therefore, the dust particles become surrounded by such a fireball before starting burning. According with this mechanism, the predictive model presented in this work proceeds through the solution of the following critical issues in order to calculate the value of the K_{St} for a given dust:

1. quantification of the effects related to the ignitors bursting in a 20 L sphere;
2. calculation of the volatiles production rate as a function of the dust properties;
3. determination of an effective flame velocity for describing the gas-phase combustion;
4. solution of the system of partial differential equations expressing all the relevant material and energy balances to calculate the maximum value of the pressure rise in the sphere, which is required to estimate the deflagration index from its standard definition (that is, the "Cubic-Root-Law").

2.1 Effects of the Ignitors Bursting

In the standard 20 L sphere the ignition source of the dust cloud is provided by two chemical ignitors (total mass equal to 2.4 g and total energy released equal to 10 kJ), which are composed by a mixture of three different powders: 30% w/w Barium Nitrate (MW=261.335 g/mol); 30% w/w Barium Peroxide (MW=169.33 g/mol); and, 40% w/w Zirconium (MW=91.22 g/mol). This is a multipoint ignition source (Zhen & Leuckel, 1996), where Barium Nitrate and Barium Peroxide decompose (practically instantaneously, total energy released: 1.586 kJ), because of the effect of a spark generated between two electrodes located inside the capsules of the chemical ignitors, to form NOx and O_2. The huge amount of Oxygen released violently scatters and oxidizes the Zirconium particles (total energy released: 8.414 kJ) which are simultaneously heated up because of the oxidation reaction and cooled down thanks to the combined effects of convection with surrounding air and radiation towards the sphere walls. A detailed modeling of such phenomena is a very hard

task because the oxidation kinetics of both nano and micro Zr particles has not been yet fully rationalized from a chemical-physical point of view. This calls for a simplified modeling of the ignitors bursting phenomenon, as discussed in the following.

A standard 20 L test was carried out without any dust inside the sphere with the aim of evaluating the contribution of the ignitors in terms of heat exchanged with the air inside the test chamber. The corresponding air temperature increase (calculated from the registered pressure vs. time trend using the ideal gas law) is about 322 °C, which corresponds to a total energy released of about 7.783 kJ. Starting from the experimental evidence that no traces of Barium Nitrate, Barium Peroxide and Zr can be found into the chamber after the ignitors bursting, it follows that there is a considerable amount of heat that is either irradiated towards the internal sphere wall or balanced by some endothermic phenomena, such as the combined heating and partial/total melting of the Zirconium particles. Basing on this observation, the following three-steps phenomenological mechanism, which tries to separate the convective phenomenon (responsible for the heating of the air inside the sphere) from both the radiating and the heating/melting phenomena, has been used: a) Barium Nitrate and Barium Peroxide decompose providing both heat and oxygen to oxidize violently the Zr particles; b) ZrO_2 is formed very rapidly, starting from the outside layer of each Zr particle, as the oxygen diffuses inside the Zr particles; c) this complex oxidation phenomenon produces incandescent hybrid particles (Zr - molten Zr and ZrO_2 – molten ZrO_2) which are cooled down by the combined effect of both convection with surrounding air and radiation towards the internal sphere walls.

Air heating can be modeled independently assuming that the unknown turbulent conditions under which the heat is transferred from the hybrid incandescent particles to the air inside the sphere can be reproduced by fitting the experimental air pressure vs. time profile obtained by detonating the ignitors inside the empty sphere. In particular, the energy balance for the air contained inside the sphere leads to the following equation:

$$\begin{cases} \rho_{air} \cdot V_{sphere} \cdot c_{p,air} \cdot \frac{dT_{air}}{dt} = \rho_{air} \cdot V_{sphere} \cdot c_{p,air} \cdot \left(\frac{V_{sphere}}{n_{air} \cdot R}\right)\frac{dP}{dt} = \frac{V_{sphere} \cdot c_{p,air} \cdot MM_{air} dP}{R \qquad dt} = Q_{ign}(t) \\ I.C. \quad t = 0, \quad T_{air} = T_{air,0} = 293K \end{cases} \quad (1)$$

where the ideal gas law has been used to relate pressure with air temperature, and $Q_{ign}(t)$ is the (unknown) power exchanged between the ignitor particles and the surrounding air at a given time from the ignition, t. The value and the shape of the unknown function $Q_{ign}(t)$ can be estimated by introducing in the l.h.s. of equation (2) the pressure vs. time experimental data obtained from a standard test in the 20 L sphere carried out without any dust and interpolating, for instance with a cubic spline, the resulting data (Fumagalli et al., 2018). Integrating $Q_{ign}(t)$ over the duration of the test leads to an estimation of the total amount of heat released to the air in the sphere equal to about 7.783 kJ; therefore, the remaining 2.217 kJ (i.e., the complement to 10 kJ) must be accounted for by both the heating/melting and radiative phenomena.

The so estimated power $Q_{ign}(t)$ should not depend, at least as a first approximation, to the presence of air only or air and dusts in the 20 L sphere; therefore, the value estimated from the experimental air pressure vs. time profile obtained by detonating the ignitors inside the sphere filled with air only will be used also for modeling the effect of the ignitors bursting during a standard test in the 20 L sphere filled with also an explosive dust.

2.2 Pyrolysis / Devolatilization Characterization

Many models for representing pyrolysis or devolatilization of solids have been proposed in the scientific literature even if they can be broadly classified in two different groups: a) models based on the assumption that the solid decomposes directly to volatiles only after reaching a critical temperature (Andrews and Atthey, 1975); b) models incorporating a kinetic mechanism for the devolatilization process which allows the solid to decompose over a characteristic temperature range. When using experimental TG data, the latter models require the use of one or more rate equations to model the weight loss of a small dust sample as a function of both the remaining mass and temperature (Staggs, 2000, Wichman, 1986, Di Blasi, 1997).

In the present work, the second approach was applied assuming a single devolatilization step through which only a part of the solid (*S*) is transformed in volatile compounds (*V*), while another portion of the solid, which can be determined using TG data (Copelli et al., 2017b), remains as char (the so-called skeleton). Such a hypothesis allows considering constant the volume of the bursting particle and, consequently, the porosity of the particle (which varies during the explosion phenomenon) can be incorporated in one of the variables. In

addition, the volatiles leave the particle as they are formed, being immediately available for the combustion process. These phenomena are represented in Figure 1.

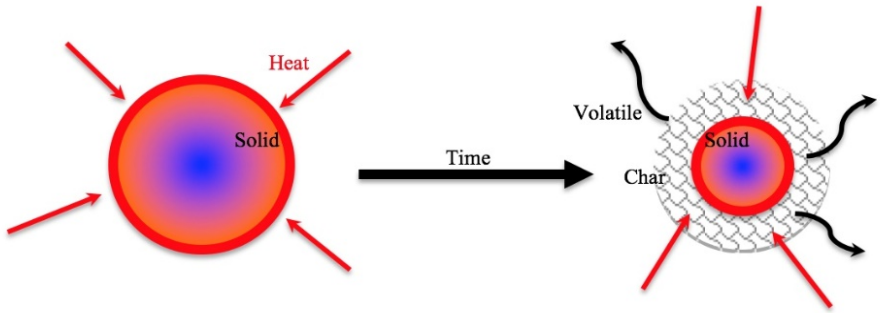

Figure 1. Sketch of a single dust particle pyrolysis mechanism.

2.1.1 Particle Material Balance on the Solid

The equations representing the consumption of the solid are based on the following assumptions: one-dimensional, spherically symmetric dust particle; negligible resistance to mass transfer and negligible diffusive flux with respect to the convective one for the gas phase; no secondary reactions of the volatile pyrolysis products; local thermal equilibrium between solid and volatiles; pseudo-steady-state assumption for the gas phase; particles with constant total volume, V_t (that is, presence of a skeleton with a constant density, ρ_S, and a non-constant porosity, ε).

As previously mentioned, the presence of a skeleton implies that not all the solid can react to give volatiles; the fate of the reacting part of the solid (that is, the part consumed by the pyrolysis/devolatilization reactions), with a mass equal to $m_{S,r}$, is described by the following material balance equation:

$$\frac{\partial m_{S,r}}{\partial t} = -r_p \cdot V_t = -k \cdot {\rho_{S,r}}^n \cdot V_t \qquad (2a)$$

where:

$$\rho_{S,r} = \frac{m_{S,r}}{V_t} = \frac{m_S}{V_t} - \frac{m_{S,0} \cdot \beta}{V_t} \qquad (2b)$$

In this last equation, β represents the non-reacting fraction of the solid, which leads to the skeleton. The value

of β for a given dust can be easily measured through a standard TG test as $\beta = \frac{m_{S,f}}{m_{S,0}}$, being $m_{S,0}$ is the initial solid mass loaded in the TG apparatus, while $m_{S,f}$ is the final solid mass detected at the end of the TG test.

By defining:

$$\rho_{S,app} = \frac{m_S}{V_t} = \frac{m_S}{V_S} \cdot \frac{V_S}{V_t} = \rho_S \cdot (1 - \varepsilon) \tag{2c}$$

$$\rho_{S,app,0} = \frac{m_{S,0}}{V_t} = \frac{m_{S,0}}{V_{S,0}} \cdot \frac{V_{S,0}}{V_t} = \rho_S \cdot (1 - \varepsilon_0) \approx \rho_S \tag{2d}$$

where $\varepsilon = \frac{V_t - V_S}{V_t} = \frac{V_V}{V_t}$ is the porosity of the dust particle (variable during the process), ε_0 is the initial porosity of the dust particle assumed equal to zero, and V_V is the volume occupied by the volatiles that they are evolved by the devolatilization process, it results:

$$\rho_{S,r} = \rho_{S,app} - \rho_{S,app,0} \cdot \beta \tag{2e}$$

Using these definitions, equation (2a) leads to:

$$\begin{cases} \frac{\partial \rho_{S,r}}{\partial t} = -k \cdot {\rho_{S,r}}^n = -A \cdot exp\left(-\frac{E_a \cdot \left(1 - \chi \cdot \left(\frac{\rho_{S,r,0} - \rho_{S,r}}{\rho_{S,r,0}}\right)\right)}{RT} \right) \cdot {\rho_{S,r}}^n \\ \quad I.C. \quad t = 0, \quad \rho_{S,r} = \rho_{S,r,0} = \rho_{S,app,0} \cdot (1 - \beta) \end{cases} \tag{2}$$

Note that a modified Arrhenius equation for representing the kinetic constant, k, has been used (Fumagalli et al., 2017), where A, E_a, n and χ are parameters to be fitted, for a given dust, on experimental data measured through a standard TG test (i.e., the same test required to measure the aforementioned β value). The fitting procedure, which is peculiar of the proposed methodology, will be discussed in more details in Section 3.

2.1.2 Particle Material Balance on the Volatiles

The material balance equation for the volatiles that are present into the gas phase of the solid dust particle (i.e., into the particle void fraction), requires to define an apparent volatiles density as:

$$\rho_{V,app} = \frac{m_V}{V_t} = \frac{m_V}{V_V} \cdot \frac{V_V}{V_t} = \rho_V \cdot \varepsilon \tag{3a}$$

which leads to the following material balance equation written into the particle spherical coordinates:

$$\frac{\partial \rho_{V,app}}{\partial t} + \frac{\partial}{\partial r}(\rho_{V,app} \cdot v_r) + \frac{2}{r} \cdot (\rho_{V,app} \cdot v_r) = k \cdot {\rho_{S,r}}^n \quad (3b)$$

Under pseudo-steady state conditions for the gaseous phase, Eq. (3b) simplifies as:

$$\frac{\partial}{\partial r}(\rho_V \cdot \varepsilon \cdot v_r) = -\frac{2}{r} \cdot (\rho_V \cdot \varepsilon \cdot v_r) + k \cdot {\rho_{S,r}}^n \quad (3c)$$

Defining the new lumped variable $\nu = \rho_V \cdot \varepsilon \cdot v_r$ [kg_G / (m^2 s)], it results:

$$\begin{cases} \frac{\partial \nu}{\partial r} = -\frac{2}{r} \cdot \nu + k \cdot {\rho_{S,r}}^n \\ B.C. \quad r = 0, \quad \nu = 0 \end{cases} \quad (3)$$

2.1.3 Particle Energy Balance

Assuming that the heat capacity of the solid phase (S) is constant and much larger than that of the gaseous phase (V), the energy balance equation on a single particle can be written as:

$$\rho_{S,eff} \cdot c_{p,S} \frac{\partial T}{\partial t} = -\nabla \times (h \cdot \vec{v} + \vec{q}) - \Delta H_p \cdot r_p \quad (4a)$$

where:

$\rho_{S,eff} = \rho_S \cdot (1 - \bar{\varepsilon})$ is an effective particle density (an effective average value of $\bar{\varepsilon}$ = 0.5 has been used); $h = \rho_{V,app} \cdot c_{p,V} \cdot T$ is the enthalpy of the volatiles per unit of volume; $\vec{q} = -\bar{\lambda} \cdot \nabla T$ is the conductive heat flux; $\bar{\lambda} = \lambda \cdot (1 - \bar{\varepsilon})$ is an effective thermal conductivity; ΔH_p is the endothermic reaction enthalpy for the pyrolysis reaction.

Using these definitions, equation (4a) can be recast in the following one:

$$\begin{cases} \rho_S \cdot (1-\bar{\varepsilon}) \cdot c_{p,S} \cdot \dfrac{\partial T}{\partial t} = \bar{\lambda} \cdot \dfrac{\partial^2 T}{\partial r^2} + \dfrac{2 \cdot \bar{\lambda}}{r} \cdot \dfrac{\partial T}{\partial r} - c_{p,V} \cdot \left[\dfrac{\partial \nu}{\partial r} \cdot T + \nu \cdot \dfrac{\partial T}{\partial r} + \dfrac{2}{r} \cdot (\nu \cdot T) \right] - \Delta H_p \cdot r_p \\ t = 0 \qquad T = T_0 = 293 \ K \\ r = 0 \qquad \bar{\lambda} \cdot \left. \dfrac{\partial T}{\partial r} \right|_{r=0} = 0 \\ r = R \qquad \bar{\lambda} \cdot \left. \dfrac{\partial T}{\partial r} \right|_{r=R} = -h_c \cdot \left(T\big|_{r=R} - T_{air} \right) - \varepsilon_{em} \cdot \sigma \cdot \left(T\big|_{r=R}{}^4 - T_{air}^4 \right) - \sigma \cdot \left(T\big|_{r=R}{}^4 - T_{ign}^4 \right) \end{cases} \quad (4)$$

where: h_c is the heat transfer coefficient (computed as discussed in (Cengel, 2008)); ε_{em} is the emissivity

(equal to 0.95); and σ is the Stefan–Boltzmann constant.

To estimate the heating of the dust particles from the hot ignitor particles (last term in the r.h.s. of the B.C. at $r = R$), the time evolution of the temperature of the ignitor particles, T_{ign}, is required. To estimate such a temperature evolution, it was hypothesized that, as the number of hybrid incandescent particles irradiating on a single dust particle is very high (of the order of 10^2 for a dust particle of about 30 μm of diameter), the ignitors behave as a sort of hot radiating cloud whose temperature varies according to the following energy balance equation on an ignitor particle:

$$\begin{cases} \rho_{Zr} \cdot V_{Zr} \cdot c_{p,Zr} \dfrac{dT_{ign}}{dt} = -\sigma \cdot A_{Zr} \cdot \left(T_{ign}^4 - T|_{r=R}{}^4\right) \\ \quad I.C. \quad t = 0, \quad T_{ign} = T_{ign,0} = 2715°C \end{cases} \tag{5}$$

Practically, it is assumed that the ignitor particles radiate directly on the dust particles external surfaces, heating them and favouring the subsequent oxidation, from an initial temperature of about 2715 °C (the ZrO_2 melting temperature).

On the other hand, to estimate the heating/cooling of the dust particles from the heat exchange with the surrounding air, the time evolution of the temperature of the air in the sphere, T_{air}, is also required. This calls for the balance equations on the whole 20 L sphere, as discussed in the following sections.

2.3 Volatiles Combustion Characterization

2.3.1 Sphere Material Balance on the Volatiles

To describe the violence of the dust explosion phenomenon it is necessary to write a material balance equation on the volatiles present into the 20 L sphere, that is, outside the dust particles. The mass flow rate of volatiles exiting from all the dust particles can be computed as:

$$m_V = v|_{r=R} \cdot \pi \cdot D_p^2 \cdot N_p \tag{6a}$$

where $v|_{r=R}$ is the massive flux of volatiles exiting from the external surface of a single dust particle; D_p is the average diameter of a dust particle (calculated from the granulometric distribution of the dust by weighting

the number of particles per granulometric class, that is, $D_p = \sum_{i=1}^{NGC} D_{p,i} \cdot f_i$); and, N_p is the number of dust particle into the sphere that can be easily computed from the dust concentration, C_D, as

$$N_p = \frac{C_D \cdot 0.02}{\rho_S \cdot \left(\frac{4}{3}\right) \cdot \pi \cdot D_p^3} \tag{6b}$$

As in this work we used a lumped combustion kinetics (see Eq. (7a)), which does not take into account for the real flammability limits, a value of C_D equal to 1 kg/m^3 has been used, which is closed to the value exhibited by most organic dusts.

The mass balance equation on the volatiles in the sphere can be written as:

$$\begin{cases} \frac{\partial \rho_V}{\partial t} = \frac{v|_{r=R} \cdot \pi \cdot D_p^2 \cdot N_p}{V_{sphere}} - k_{c,T} \cdot \rho_V \\ I.C. \quad t = 0, \quad \rho_V = 0 \end{cases} \tag{6}$$

where ρ_V is the concentration of volatiles inside the sphere. We can see that volatiles are generated by devolatilization from the dust particles (first term in the r.h.s. of the previous equation) and they are consumed by the gas phase combustion (second term in the r.h.s. of the previous equation), here supposed to occur through a lumped first order reaction kinetics The combustion kinetic constant, $k_{c,T}$, can be estimated as a function of the characteristic time of the homogeneous combustion step, t_c, as:

$$k_{c,T} = \frac{1}{t_c} \tag{7a}$$

The characteristic combustion time can be roughly estimated as:

$$t_c = \frac{\delta}{S} \tag{7b}$$

where δ is the flame thickness, normally of the order of 0.5-1 mm (Di Benedetto et al., 2010) and *S* is the turbulent burning velocity of the volatiles, which in turn can be estimated as (Zhen and Leuckel, 1996):

$$S = S_{lam} \cdot \left(1 + 3.5 \frac{u'^{0.5}}{S_{lam}}\right) \tag{7c}$$

where S_{lam} is the laminar burning velocity of the combustible gases and *u'* is the velocity fluctuation. The latter was estimated to be, in the 20 L sphere after the usual delay time of 60 ms (Hertzberg, Cashdollar, 1987), equal to about 2.68 m/s (Dahoe et al., 2001).

For calculating the laminar burning velocity of the combustible gases, the composition of the volatiles should be estimated. However, considering that, for most of the organic dusts, methane is the most abundant pyrolysis product and that even relevant amount of hydrogen (which could be produced in the pyrolysis/devolatilization step) do not alter in a significant way the methane laminar burning velocity (Wang et al., 2015), the laminar burning velocity of methane in stoichiometric conditions was used in equation (7c).

2.3.2 Sphere Energy Balance on the Gas Phase

Assuming uniform gas phase temperature; negligible amount of pyrolyzed/combustion gases into the sphere with respect to the air introduced during the dust inlet; and all the dust particles bursting at the same time inside the sphere (coherently with the assumption of a fireball-like behavior of the ignitors bursting), the energy balance equation for the gases into the 20 L sphere becomes:

$$\begin{cases} \rho_a \cdot V_{sphere} \cdot c_{p,a} \cdot \frac{dT_{air}}{dt} = Q_{ign} + \Delta H_c \cdot k_{c,T} \cdot \rho_V \cdot V_{sphere} + \\ h_c \cdot A_p \cdot N_p \cdot \left(T|_{r=R} - T_{air}\right) + \varepsilon_{em} \cdot \sigma \cdot N_p \cdot \left(T|_{r=R}{}^4 - T_{air}^4\right) \\ I.C. \quad t = 0, \quad T_{air,0} = 293K \\ A.C. \qquad Q_{ign} = Q_{ign}(t) \end{cases} \tag{7}$$

where: ΔH_c is the enthalpy of the homogeneous combustion reaction; and $Q_{ign}(t)$ is the power exchanged between air and ignitors particles, as previously discussed.

Note that Eq. (7) is similar to Eq. (1); in addition to the power introduced by the ignitors bursting, the power arising from the homogeneous combustion and both the radiative and convective powers due to heat exchanged between the air and the external surfaces of all the dust particles have been included.

2.4 Deflagration Index Calculation

The previously discussed equations (from Eq. (2) to Eq. (7)) represent a system of 6 mixed algebraic and

partial/ordinary differential equations in the 6 dependent variables: $\rho_{S,r}$, ρ_V, v, T, T_{air}, and T_{ign} as a function of time, *t*, and dust particle radial coordinate, *r*. Such a system of equations was numerically solved using the Method Of Lines (MOL) (Schiesser, 1991) with the spatial derivatives approximated using a simple constant step, five-point centered finite difference scheme (Vande Wouver et al., 2004). This allows computing not only the values of all the dependent variables along a standard test in the 20 L sphere for a given dust, but also the value of $(dT/dt)_{max}$ for such a test. Such a value can be related (using the ideal gas law) to the value of the deflagration index through its standard definition:

$$K_{St} = \left(\frac{dP}{dt}\right)_{max} \cdot V_{sphere}{}^{1/3} = \left(n_a \cdot \frac{R}{V_{sphere}}\right) \cdot \left(\frac{dT_{air}}{dt}\right)_{max} \cdot V_{sphere}{}^{1/3} \quad (8)$$

Note that the proposed approach for the K_{St} calculation is fully predictive since the only experimental data required arise from a standard TG test.

3. Results and discussion

The present model for the deflagration index prediction was validated using experimental data of eight different organic dusts, namely: Aspirin, Cork, Corn starch, Niacin, Polyethylene, Polystyrene, Sugar, and Wheat Flour. As it is possible to notice from Eq. (2) to Eq. (7), the mathematical model involves some constitutive parameters, namely:

1. Chemical-physical parameters:

- MM, average molecular mass of the volatiles
- λ, effective thermal conductivity of the dust
- ρ_S, density of the dust
- $c_{p,S}$, specific heat of the solid
- $c_{p,V}$, specific heat of the volatiles
- ΔH_c, enthalpy of combustion
- ΔH_p, enthalpy of devolatilization/pyrolysis

2. Geometric parameters:

- D_p, average diameter of the dust particle

3. Kinetic parameters:

- A, pre-exponential factor of the lumped pyrolysis reaction
- E_{att}, activation energy of the lumped pyrolysis reaction
- n, order of the lumped pyrolysis reaction
- χ, modifier of the activation energy
- β, residue at the end of a TG analysis.

While the chemical-physical parameters have been either taken from the literature or calculated using a suitable software as summarized in Table 1, the kinetic parameters have been estimated using equation (2) to reproduce TG curves for mass loss data from the literature. For each dust, the fitting procedure was carried out through the standard least square method using only the experimental data up to the maximum slope (i.e., before any inflection point) of the TG curve. This is a key point for the correct prediction of the deflagration index value, which is related to the maximum rate of the volatile production. This means that whatever the solid residue behavior is after the maximum rate of volatiles expulsion does not contribute to the determination of the K_{St}; therefore, the corresponding part of the TG curve can be neglected. For example, Figure 2 (LINSEIS Messgeräte, official website) shows the mass loss curve vs. temperature which was used to estimate the Aspirin pyrolysis kinetic parameters. First of all, the residue at the end of the TG test, β, can be directly estimated from the mass loss curve at the final test temperature (e.g. 600 °C) equal to about 3.7. The other pyrolysis kinetic parameters were estimated by fitting equation (2) to the first part of the experimental TG curve, that is, until the occurrence of the maximum rate of weight loss (indicated in Figure 2 with the symbol α) which occurred at about 177 °C.

Table 1. Physical-chemical properties for all the investigated dusts ([a] estimated with Chetah® software; a discussion of the reliability of Chetah® Software is reported elsewhere, Pasturenzi et al., 2014).

	Aspirin **(NIST, Fisher Scientific, Kirklin, 1999)**	**Cork** **(Scholar Chemistry, 2008, Silva et al., 2013, Engineering Toolbox, Imperial Cork, official website, 2018, Xu and Ferdosian, 2017)**	**Corn starch** **(Sciencelab, Hwang et al., 1999)**	**Niacin** **(Sciencelab, Agreda, 2007)**	**Polyethylene** **(Dow chemicals, 2013, Rabinovitch, 1965, Staggs, 2000, Di Blasi, 1997, Chemèo)**	**Polystyrene** **(NIST, Di Blasi, 1997)**	**Sugar** **(Sciencelab, IPCS, 2003, Anderson et al., 1950, Di Blasi, 1997, Maccarthy and Fabre, 1989)**	**Wheat flour** **(NIST, Berton et al., 2002, Di Blasi, 1997)**
MM, **g/mol**	180.159	164.05	180.156	123.111	28.05	104.1491	342.297	120.1
ρ_S, **kg/m³**	1400	250	1480	1162	920	1040	1590	527
$c_{p,S}$, **J/(kg K)**	893.10	350	1631	1243	2300	1800	1263	2500
$c_{p,V}$, **J/(kg K)**	2125	1900	2125	2125	2500	2500	2500	2500
λ, **W/(m K)**	0.165	0.045	0.167	1	0.01	0.02	0.167	0.075

ΔH_c, **J/kg**	2.18 x10^7	2.93x10^7	1.56x10^{7a}	2.22x$10^{7\,a}$	5.03x10^7	4.22 x$10^{7\,a}$	8.18 x$10^{6\,a}$	1.83 x$10^{7\,a}$
ΔH_p, **J/kg**	-3.51x10^5	-1.52x10^6	-8.00x10^{5a}	-2.02E x$10^{5\,a}$	-9.60 x$10^{5\,a}$	-6.39 x$10^{5\,a}$	-4.00 x$10^{5\,a}$	-8.00 x$10^{5\,a}$

Table 2 – Pyrolysis kinetic parameters for all the investigated dusts

Parameter	***Aspirin***	***Cork***	***Corn Starch***	***Niacin***	***Polyethylene***	***Polystyrene***	***Sugar***	***Wheat Flour***
E_a, ***J/mol***	1.425x10^5	1.114 x10^5	2.220 x10^5	1.328 x10^5	1.844 x10^5	1.792 x10^5	3.574 x10^5	1.861 x10^5
A,	1.546 x10^{11}	2.394 x10^{11}	3.270 x10^9	9.553 x10^{14}	6.578 x10^{14}	4.228 x10^{14}	7.357 x10^{14}	4.012 x10^{14}
n	3.09	0.862	4.54	0.94	0.665	0.821	8.16	1.867
χ	-0.154	-0.183	0.158	0.0124	0.0887	0.124	-0.1112	0.236
β	0.0369	0.0487	0.1101	9.40 x10^{-6}	0.0142	0.0705	0.207	0.1101

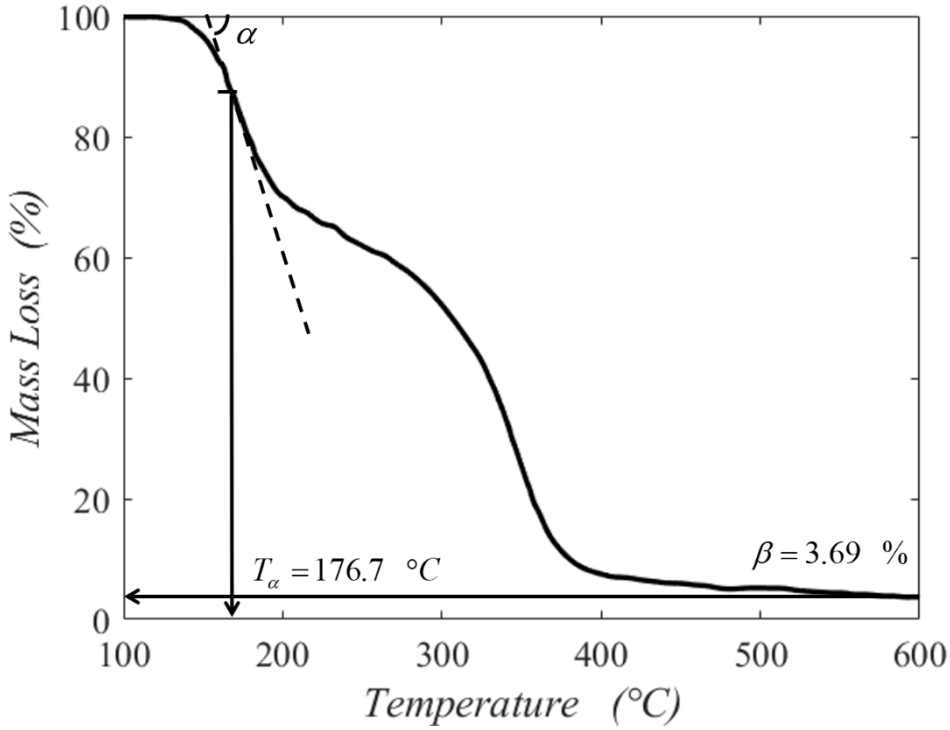

Figure 2 – Weight loss vs. Temperature TG curve for Aspirin (Data Source: LINSEIS Messgeräte. Official website)

Figures from 3A to 3H show a comparison between experimental and fitted data in terms of conversion vs. Temperature curves. Conversion is defined as $\zeta = \frac{\rho_{S,r,0} - \rho_{S,r}}{\rho_{S,r,0}}$, where the values of $\rho_{S,r}$ as a function of time can be derived from the experimental data of mass loss as a function of time or predicted by solving Eq. (2) enforcing a constant heating rate. It is important to clarify that all the TG tests (both literature and our experimental ones) were carried out using the same heating rate (that is, 10 °C/min). Differences related to the nitrogen flux used or the TG device were considered not significant for the point of view of the determination of the pyrolysis kinetics. A possible limitation of this approach can be traced in diffusional problems through the dust layer inside the TG apparatus (Fang et al. 2017). Precisely for this reason, in this work a very large TG crucible, loaded with the smallest possible amount of dust, has been used. Using this shrewdness, possible diffusional limitations through the dust layer are largely reduced and they can be neglected.

We can see that all the experimental TG curves are reasonably well fitted in the investigated temperature range.

The estimated kinetic parameters for the eight dusts are summarized in Table 2.

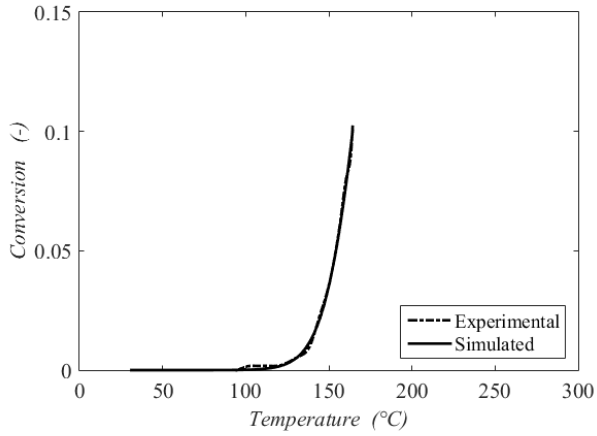

A

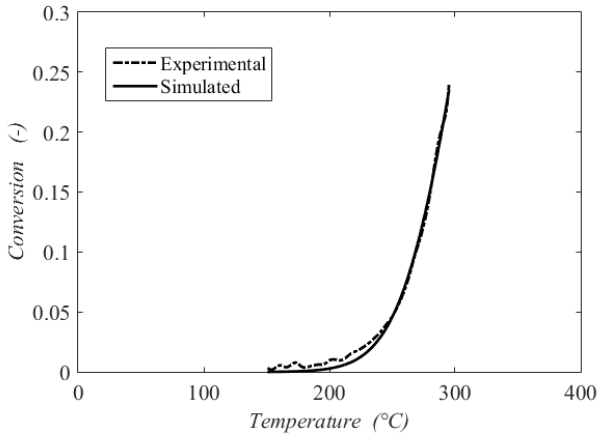

B

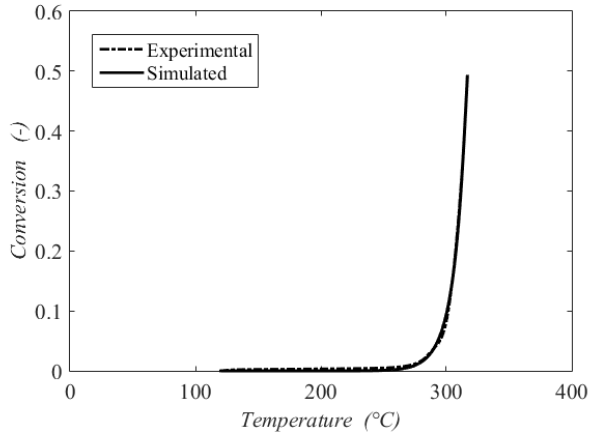

C

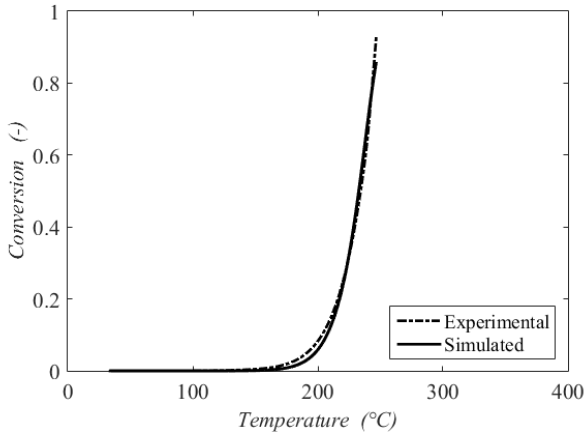

D

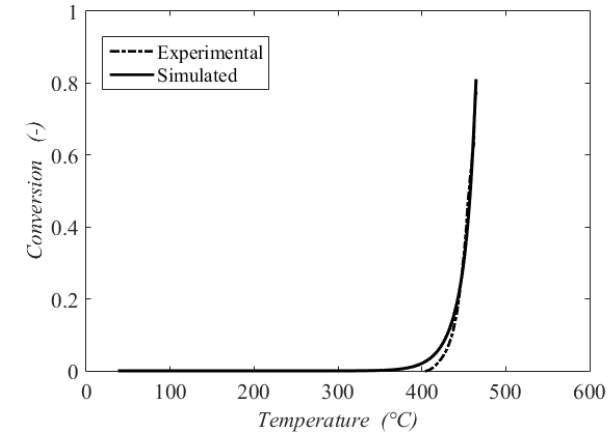

E

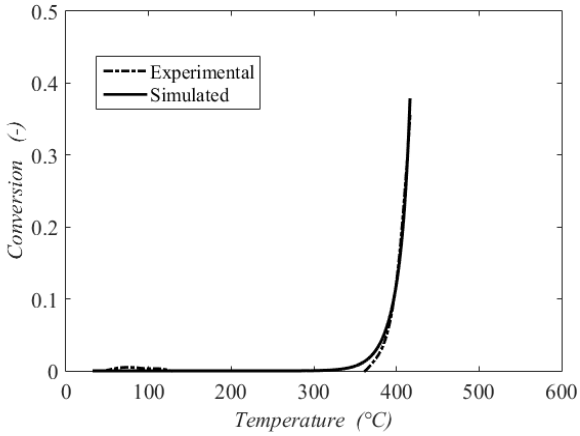

F

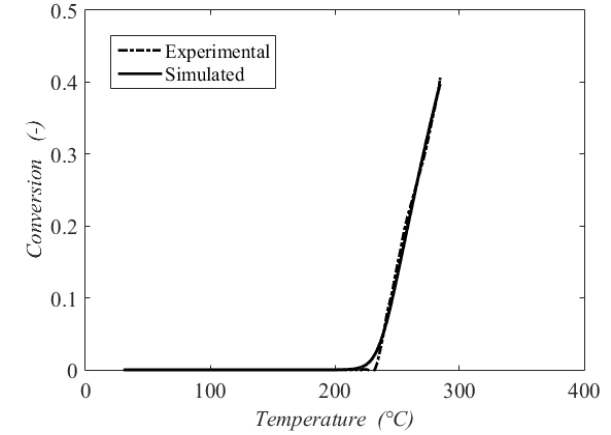

G

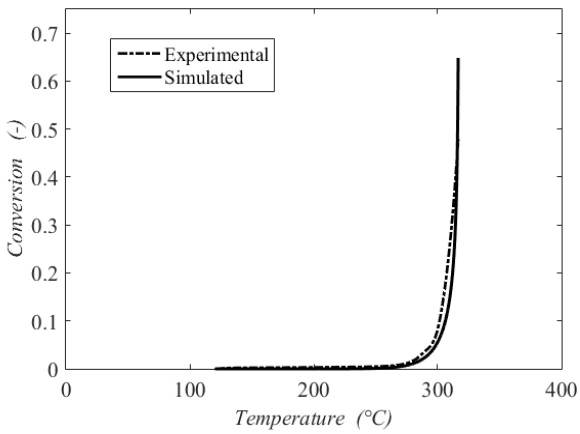

H

Figure 3 – Conversion vs. Temperature curves for: A) Aspirin (source: LINSEIS Messgeräte GmbH); B) Cork (source: Şena et al., 2014); C) Corn Starch (our experimental data); D) Niacin (our experimental data); E) Polyethylene (source: Contat-Rodrigo et al., 2002); F) Polystyrene (experimental data from (source: Özsin and Eren Pütün, 2017)); G) Sugar (our experimental data); H) Wheat flour (our experimental data). All our experimental data have been obtained using a SDT Q600 V8.3 Build 101 DSC-TGA, a temperature ranging from 35 to 700 °C, a Heating Rate of 10 °C/min and a Nitrogen Flux of 100 mL/min.

Using the parameters summarized in Tables 1 and 2, the mathematical model previously discussed has been solved numerically to predict the K_{St} values for the eight dusts considered. Such predicted values are compared with the experimental data in Table 3. We can see that the proposed approach is able to predict the experimental values quite reasonably. However, it should be noted that among all the parameters involved in the mathematical model, λ plays a relevant role: this behavior has been found to be true in the work of Fumagalli et al. (2017) and it can be derived from a comparison among the characteristic times of the dust explosion process that act on the K_{st} determination (that is, external heat transfer, internal heat transfer, pyrolysis or devolatilization, and homogeneous combustion). Even in this work it was confirmed that the rate determining steps in defining the violence of a dust explosion in the 20 L sphere test are mainly related to the particle heating: that is, either internal or external heat transfer. Table 3 also reports the values of the Biot numbers for each dust, giving a clear indication on the effective rate determining step between internal or external heat transfer. In this study it also true that, being the external heat transfer conditions practically the same from one test to another (for all dusts the methane turbulent burning velocity has been used to calculate h_c), λ is the only parameter that really affects the K_{st} value.

The comparison among experimental and predicted K_{st} values is also reported in the parity plot of Figure 4, from which it is possible to see that all the predicted deflagration indexes are always in the accepted range of uncertainty. The error bar have been assigned according to the range of K_{St} value: e.g., when the K_{St} is over 200 bar/(m s), the corresponding error bar will be 20%; when it comprised between 100 and 200 bar/(m s), it will be 15%; and, finally, when it is lower than 100 bar/(m s), it will be 10% (ISO, 1985).

Table 3: Experimental vs. predicted Kst values

Dust	***D_p (Weighted Average) [µm]***	***Bi [-]***	***$K_{st\ EXP}$ [bar m/s]***	***$K_{st\ MOD}$ [bar m/s]***
***Aspirin* (Eckhoff, 2003)**	25	6.00e-1	217	220
***Cork* (NFPA, 2013)**	42	2.53e+0	202	200
***Corn starch* (Fumagalli et al., 2017)**	54	7.36e-1	132	131
***Niacin* (Fumagalli et al., 2017)**	37	1.10e-1	215	220
***Polyehtylene* (Di Blasi, 1997)**	28	1.03e+1	133	147
***Polystyrene* (NFPA, 2013)**	20	4.72e+0	218	216
***Sugar* (NFPA, 2013)**	37	6.22e-1	138	155
***Wheat flour* (Fumagalli et al., 2017)**	57	1.67e+0	62	63

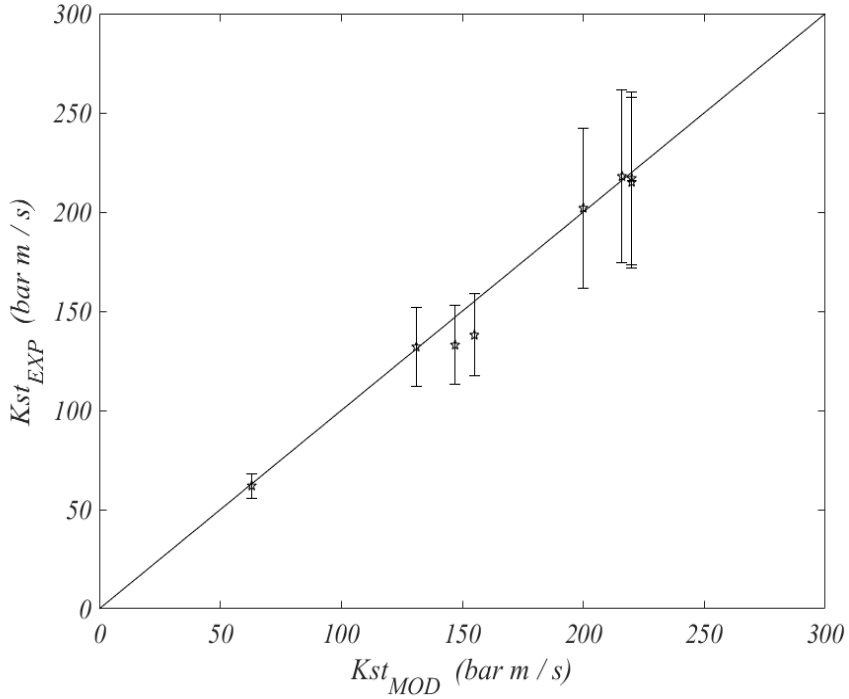

Figure 4 - Comparison among model and experimental values of K_{St}. See Table 3 for the sources of the experimental data.

4. Conclusions

The original purpose of this work was to develop a quite simplified mathematical model able to predict the K_{St} value of organic dusts (as it would be obtained from a standard 20 L sphere test) using only experimental data from thermo-gravimetric tests. The proposed approach was validated by comparison with experimental values measured in a 20 L sphere for eight common organic dusts: Aspirin, Cork, Corn starch, Niacin, Polyethylene, Polystyrene, Sugar, and Wheat flour.

The results can be considered quite promising as the developed model allows for predicting quite reasonably the K_{St} value for different dusts with different particles size. Of course, this predictive model needs further validations before being used without concerns. Therefore, an experimental test in the 20 L sphere still remains, actually, the most appropriate and safest way to measure the deflagration index.

Anyway, this approach could allow for a substantial reduction of time and costs, making the evaluation of the risks linked to combustible dusts much more affordable.

Nomenclature

A	Pre-exponential factor, [1/s]
A_p	Surface area of a particle dust, [m²]
A_{Zr}	Surface area of Zirconium particle, [m²]
C_D	Concentration of dust particles inside the 20 L sphere, [kg/m³]
$c_{p,air}$	Specific heat of the gas phase, [J/(kg·K)]
$c_{p,V}$	Specific heat of volatiles, [J/(kg·K)]
$c_{p,Zr}$	Specific heat of Zirconium, [J/(kg·K)]
D_p	Average Particle Diameter, [m]
E_a	Activation energy, [J/mol]
f	Fraction of particles belonging to a given granulometric class, [-]
h	Enthalpy of volatiles per unit of volume, [J/m³]
h_c	Heat transfer coefficient, [W/(m²·K)]
ΔH_p	Combustion heat, [J/kmol]
ΔH_p	Pyrolysis reaction heat, [J/kmol]
k	Pyrolysis kinetic constant, [1/s]
$k_{c,T}$	Combustion kinetic constant, [1/s]
K_{st}	Deflagration index [bar/(m·s)]
$m_{S,0}$	Total mass of dust loaded, [kg]
$m_{S,f}$	Dust mass at the end of the test, [kg]
$m_{S,r}$	Mass of dust that reacts, [kg]
n	Order of reaction, [-]
N_p	Number of particles, [-]
P	Pressure, [Pa]
P_{max}	Maximum pressure, [Pa]

Q_{ign}	Convection heat due to the combustion of ignitors, [W]
q	Conductive heat flux, [W/m²]
R	Ideal gas constant, [J/(mol·K)]
S	Solid phase
	Turbulent burning speed, [m/s]
S_{lam}	Laminar burning speed, [m/s]
r	Particle radius, [m]
r_p	Pyrolysis reaction rate, [mol/(m³·s)]
t	Time, [s]
t_c	Characteristic time of homogeneous combustion, [s]
T	Particle temperature, [K]
T_{air}	Temperature of the gas in the vessel, [K]
T_{ign}	Temperature of ignitors, [K]
T_{wall}	Temperature of the vessel wall, [K]
T_{Zr}	Temperature of a Zirconium particle, [K]
u'	Velocity fluctuation, [m/s]
V_{Sphere}	Vessel volume, [m³]
V	Volatiles
V_S	Volume of loaded solid dust, [m³]
V_t	Particles Volume, [m³]
V_V	Volatiles Volume, [m³]
V_{Zr}	Volume of Zirconium particle, [m³]

air	Referred to gas phase
app	Apparent parameter
eff	Effective parameter
max	Maximum
NGC	Number of Granulometric Classes (for a given dust sample)
S	Referred to as solid phase (dust)
Sphere	Referred to as apparatus volume, where the explosion takes act
V	Referred to as volatiles phase
0	Referred to initial conditions, starting time

Greek symbols

β	Fraction of dust residual, [-]
δ	Flame thickness, [m]
ε	Void fraction, [-]
ε_{em}	Emissivity, [-]
ν	Volatiles mass flux, [kg/(m²·s)]
ν_r	Volatiles outlet velocity, [m/s]
λ	Thermal conductivity, [W/(m·K)]
ζ	Conversion, [-]
ρ_{air}	Gas phase density, [kg/m³]
ρ_S	Dust density, [kg/m³]
$\rho_{S,app}$	Apparent dust density, [kg/m³]
$\rho_{S,r}$	Density inside the particle, referred to the volume effectively involved in the combustion, [kg/m³]
ρ_V	Volatiles density, [kg/m³]
$\rho_{V,app}$	Apparent volatiles density, [kg/m³]

ρ_{Zr}	Zirconium density, [kg/m³]
χ	Correction factor for activation energy, [-]
σ	Stefan-Boltzmann constant, [W/(m²·K⁴)]

REFERENCES

Agreda, A.G., 2007. Explosion of dust/gas hybrid mixture. Ingegneria Chimica, dei materiali e della produzione, Università degli Studi di Napoli Federico II, PhD Thesis.

Anderson, G.L., Higbie, H., Stegeman, G., 1950. The heat capacity of sucrose from 25 to 90°C. Journal of the American Chemical Society 72 (8), pp. 3798-3799.

Andrews, J.G., Atthey, D.R, 1975. On the motion of an intensely heated evaporating boundary. IMA Journal of Applied Mathematical 15(1), pp. 59-72.

Bartknecht, W., 1971. Brenngasund Staubexplosionen. Forschungsbericht F45. Koblenz: Bundesinstitut fur Arbeitsschutz.

Bartknecht, W., 1978, Explosionen-Ablauf und Schutzmassnahmen. Berlin: Springer-Verlag.

Bartknecht, W., 1981. Explosions: Course, Prevention, Protection. Springer- Verlag, Berlin.

Beidaghy Dizaji, H., Faraji Dizaji, F., Bidabadi, M., 2014. Determining thermo-kinetic constants in order to classify explosivity of foodstuffs. Combustion. Explosion and Shock Waves 50 (4), pp. 454-462.

Berton, B., Scher, J., Villieras, F., Hardy, J., 2002. Measurement of hydration capacity of wheat flour: influence of composition and physical characteristics. Powder Technology 128 (2-3), pp. 326-331.

Cashdollar, K.J., Hertzberg, M., Zlochower, I.A, 1989. Effect of volatility on dust flammability limits for coals, gilsonite, and polyethylene. Proceedings of the 2nd Symphosium (Int.) Combust. 22 (1), pp. 1757-1765.

Cengel, Y.A, 2008. Introduction to Thermodynamics and Heat Transfer, 2nd Edition. Mc Graw Hill.

Cloney, C., 2017 Combustible Dust Incident Report – Version #1, (2018) Retrieved from http://www.myDustExplosionResearch.com/2017-Report. (accessed: 1 September 2018).

Contat-Rodrigo, L., Ribes-Greus, A., Imrie, C.T., 2002. Thermal Analysis of High-Density Polyethylene and Low-Density Polyethylene with Enhanced Biodegradability. Journal of Applied Polymer Science 86, pp. 764–772.

Copelli, S., Raboni, M., Ragazzi, M., Rada, E.C., Torretta, V., 2017a. Variation of the explosion risk in a hybrid collector during revamping operations. International Journal of Safety and Security Engineering 7 (2), pp. 113-125.

Copelli, S., Fumagalli, A., Gigante, L., Pasturenzi, C., 2017b. Synthesis of tin (II) sulfide: Determination of the reaction kinetics through calorimetric techniques. Powder Technology 311, pp. 416-425.

Dahoe, A.E., Cant, R.S., Scarlett, B., 2001. On the decay of turbulence in the 20-liter explosion sphere. Flow Turbul Combust 67, pp. 159–184.

Di Benedetto, A., Russo, P., Amyotte, P., Marchand, N., 2010. Modelling the effect of particle size on dust explosions. Chemical Engineering Science 65 (2), pp. 772-779.

Di Blasi, C. 1997. Linear pyrolysis of cellulosic and plastic waste. Journal of Analytical and Applied Pyrolysis, PYROLYSIS '96 40-41, pp. 463-79.

Dow Chemicals, 2013. SdS Polyethylene. Available at: https://www.dow.com/en-US/ShowPDF.ashx?id=090003e880725934. (accessed: 1 September 2018).

Eckhoff., R.K., 2003. Dust Explosions in the Process Industries, 3rd ed. Gulf Professional Publishing.

Engineering ToolBox, 2003. Specific Heat of Solids. Available at: https://www.engineeringtoolbox.com/specific-heat-solids-d_154.html. (accessed: 1 September 2018).

Ethylene (CAS 74-85-1) - Chemical & Physical Properties by Cheméo. Available at: https://www.chemeo.com/cid/56-863-2/Ethylene. (accessed: 1 September 2018).

Fang, Y., Zou, R., Luo, G., Chen, J., Li, Z., Mao, Z., Zhu, X., Peng, F., Guo, S., Li, X., Yao, H., 2017. Kinetic Study on Coal Char Combustion in a Microfluidized Bed. Energy and Fuels 31 (3), pp. 3243-3252.

Fischer scientific, official website, 2015. Available at: https://beta-static.fishersci.com/content/dam/fishersci/en_US/documents/programs/education/regulatory-documents/sds/chemicals/chemicals-a/S25122.pdf (accessed: 1 September 2018)

Fumagalli, A., Derudi, M., Rota, R., Copelli, S., 2016. Estimation of the deflagration index K_{St} for dust explosions: a review. J. Loss Prev. Process Industries 44 (1), pp. 311-322.

Fumagalli, A., Derudi, M., Rota, R., Snoeys, J., Copelli. S., 2017. Prediction of the deflagration index for organic dusts as a function of the mean particle diameter. Journal of Loss Prevention in the Process Industries 50, pp. 67-74.

Fumagalli, A., Derudi, M., Rota, R., Snoeys, J., Copelli, S., 2018. A kinetic free mathematical model for the prediction of the K_{st} reduction with the particle size increase. Journal of Loss Prevention in the Process Industries 52, pp. 93-98.

Hertzberg, M., Cashdollar, K.L., 1987. Introduction to Dust Explosions. In Industrial Dust Explosions, ed. K. L. Cashdollar and M. Hertzberg. ASTM Special Technical Publication 958. Philadelphia: ASTM, pp. 5-32.

Hertzberg, M., Zlochower, I.A., 1990. Devolatilization rates and interparticle wave structures during the combustion of pulverized coals and poly-methlmethacrylate. Symposium (Int.) Combust. 23, pp. 1247-1255.

Hwang, C.H., Heldman, D.R., Chao, R.R., Taylor, T.A., 1999. Changes in specific heat of corn starch due to gelatinization. Journal of Food Science 64 (1), pp. 141-44.

Kirklin, D.R., 1999. Enthalpy of combustion of acetylsalicylic acid. The Journal of Chemical Thermodynamics 32, pp. 701-709.

International Standards Organization, 1985. Explosion Protection Systems- Part 1: Determination of Explosion Indices of Combustible Dusts in air. International Standard ISO DIS 6184/1.Geneva:ISO.

International Chemical Safety Card 1507 (ICSC). Sucrose. International Programme on Chemical safety, Geneva, 2003.

LINSEIS Messgeräte GmbH, official website. Available at: https://www.pragolab.cz/documents/2_TGA_PT_1000_ENG.pdf. (accessed: 1 September 2018)

Maccarthy, D.A., Fabre, N., 1989. Thermal conductivity of sucrose. Chapter of Food Properties and Computer-Aided Engineering of Food Processing Systems, Vol. 168 of the series NATO ASI Series, pp. 105-111.

National Fire Protection Association, 2013. In: Standard on Explosion Protection by Deflagration Venting, vol. 68, NFPA.

NIST Website Chemistry, WebBook. Available at: https://webbook.nist.gov/cgi/cbook.cgi?ID=C50782&Type=THZ-IR-SPEC&Index=0 (accessed: 1 September 2018).

Özsin, G., Eren Pütün, A., 2017. Insights into pyrolysis and co-pyrolysis of biomass and polystyrene: Thermochemical behaviors, kinetics and evolved gas analysis. Energy Conversion and Management 149, pp. 675–685.

Pasturenzi, C., Dellavedova, M., Gigante, L., Lunghi, A., Canavese, M., Cattaneo, C.S., Copelli, S., 2014. Thermochemical stability: A comparison between experimental and predicted data. Journal of Loss Prevention in the Process Industries 28, pp. 79-91.

Properties of Cork. Imperial Cork. Manufacturing Cork Stoppers website, 2018. Available at: http://www.imperialcork.com/en/products/properties-of-cork. (accessed: 1 September 2018).

Rabinovitch, B., 1965. Regression rate and the kinetics of polymer degradation. In: Proceedings of 10th Symposium (Int.) on Combust. The Combustion Institute, Pittsburgh, pp. 1395-1397.

Siwek, R., 1977. 20-L-Laborapparaturfur die Bestimmung der Explosionskenngrossen brennbarer Staube. Diploma thesis. Technical University of Winterthur, Switzerland.

Schiesser W.E., 1991 The numerical method of lines: Integration of Partial Differential Equations, Academic Press, San Diego.

Scholar chemistry, official website, 2008. Available at: https://www.mccsd.net/cms/lib/NY02208580/Centricity/Shared/Material%20Safety%20Data%20Sheets%20_MSDS_/MSDS%20Sheets_Cork_Dust_233_00.pdf. (accessed: 1 September 2018).

Sciencelab, official website. Corn Starch SDS. Available at: http://www.sciencelab.com/msds.php?msdsId=9925088. (accessed: 1 September 2018).

Sciencelab, official website. Niacin SDS. Available at: http://www.sciencelab.com/msds.php?msdsId=9926207. (accessed: 1 September 2018).

Sciencelab, official website. Sucrose SDS Available at: http://www.sciencelab.com/msds.php?msdsId=9927285. (accessed: 1 September 2018).

Şena, A., Van den Bulcke, J., Defoirdt, N., Van Acker, J., Pereira, H., 2014. Thermal behaviour of cork and cork components. Thermochimica Acta 582, pp. 94–100.

Silva, S.P., Sabino, M.A., Fernandes, E.M., Correlo, V.M., Boesel, L.F., Reis, R.L., 2013. Cork: properties, capabilities and applications. International Materials Reviews 50(6), pp. 346-365.

Siwek, R., 1988. Zuverlassige Bestimmung explosionstechnischer Kenngrossen in der 20-Liter Laborapparatur. VDZ-Berichte 701, pp. 215-262.

Staggs, J.EJ., 2000. A simple model of polymer pyrolysis including transport of volatiles. Fire Safety Journal 34 (1), pp. 69-80.

Styrene, Oligomers. Website NIST Chemistry WebBook. Available at: https://webbook.nist.gov/cgi/cbook.cgi?ID...Contrib... (accessed: 1 September 2018).

Vande Wouwer, A., Saucez P., Schiesser, W.E., 2004. Simulation of distributed parameter systems using a Matlab-based method of lines toolbox: Chemical engineering applications. Industrial and Engineering Chemistry Research 43, pp. 3469-3477.

Xu, C., Ferdosian, F., 2017. Degradation of Lignin by Pyrolysis, in: Conversion of Lignin into Bio-Based Chemicals and Materials, Springer-Verlag GmbH, Germany, pp. 13-33. Available at: https://www.springer.com/cda/content/document/cda_downloaddocument/9783662549575-c2.pdf?SGWID=0-0-45-1608533-p180855316. (accessed: 1 September 2018).

Wang, M., Zhongsheng, L., Wenbiao, H., Jinxiu, Y., Haitao, X., 2015. Coal pyrolysis characteristics by TG-MS and its late gas generation potential. Fuel 156, pp. 243-253.

Wheat flour. Website Ensciencelabs.com. Available at: http://www.esciencelabs.com/sites/default/files/msds_files/Flour.pdf. (accessed: 1 September 2018).

Wichman, I.S., 1986. A model describing the steady-state gasification of bubble-forming thermoplastics in respone to an incident heat flux. Combust. Flame 63 (1-2), pp. 171-229.

Zhen, G., Leuckel, W., 1996. Determination of Dust-Dispersion-Induced Turbolence and its influence on dust explosions. Combustion Science and technology 113 (1), pp. 629-639.